Dipole Strength Function in ^{20}O

E. Tryggestad,[a,b] T. Aumann,[a,*] D. Bazin,[a] J. R. Beene,[c] Y. Blumenfeld,[a,†]
M. Chartier,[a,c,‡] M. L. Halbert,[d] P. Heckman,[a,b] J. F. Liang,[e] D. C. Radford,[c]
D. Shapira,[c] B. M. Sherrill,[a,b] M. Thoennessen,[a,b] and R. L. Varner[c]

[a]National Superconducting Cyclotron Laboratory,
Michigan State University, East Lansing, MI, 48824

[b]Michigan State University, Department of Physics and Astronomy,
East Lansing, MI 48824

[c]Physics Division, Oak Ridge National Laboratory, Oak Ridge, TN 37831

[d]University of Tennessee, Knoxville, TN 37996

[e]Oak Ridge Associated Universities, Oak Ridge, TN 37831

The dipole strength function of neutron-rich ^{20}O was measured in the region of 1 to 8 MeV by the method of virtual photon scattering. This method relies on the detection of real decay-photons following the virtual excitation of relativistic projectiles. A 100 MeV/u ^{20}O beam was excited by a ^{208}Pb target and the energy-loss of the projectile was correlated with the γ-ray energies. The observed ^{20}O excitation spectrum shows several broad peaks in the region above 3 MeV, which indicates a shifting of low-lying dipole strength from higher excitation energies in this neutron-rich oxygen isotope.

1. INTRODUCTION

The investigation of collective modes in unstable nuclei has recently become an important topic in the study of exotic nuclei. The isovector giant dipole resonance (GDR) is one of the most important and easily accessible of these collective modes. Theoretical calculations predict that GDR strength in neutron-rich nuclei will shift towards lower excitation energies as one probes closer to the neutron dripline [1,2].

As an example, Figure 1 shows experimental $(\gamma, x\mathrm{n})$ scattering data for the β-stable oxygen isotopes ^{16,17,18}O [3]. Specifically, one can observe a relative increase of GDR strength at lower excitation energies in ^{18}O. The present experiment was performed to extend the scope of experimental knowledge regarding dipole strength in the oxygen isotopes. Studying neutron-rich ^{20}O, though, requires the use of radioactive beams and involves the excitation of the projectile rather than the target.

*Permanent address: GSI, Planckstr. 1, 64291 Darmstadt, Germany
†Permanent address: IN_2P_3-CNRS, 91406 Orsay Cedex, France
‡Permanent address: CEN Bordeaux-Gradignan, BP 120, 33175 Gradignan Cedex, France

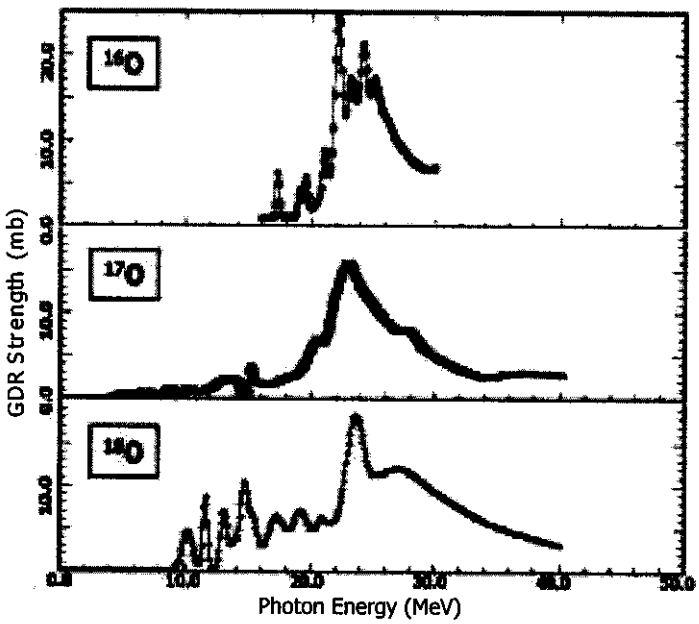

Figure 1. GDR strength distribution in oxygen isotopes measured by $(\gamma, x\mathrm{n})$ scattering. Significant strength is shifted towards lower energies for the neutron-rich isotopes (adapted from [3].)

Two alternative experimental methods have been proposed, both of which rely on the Coulomb excitation of the projectile. The first of these is virtual photon absorption, where the excitation energy of the projectile is reconstructed knowing the energies of the break-up fragment and neutron(s) [4,5]. The second technique, explored in this study, is virtual photon scattering, a method which relies exclusively on projectile γ-ray decays [6]. Presently, low beam intensities constrain studies with neutron-rich, exotic nuclei, thereby limiting them to the light mass region. Therefore, the present experiment to measure the GDR strength function in ^{20}O also served as a test for the feasibility of the method.

2. VIRTUAL PHOTON SCATTERING

The experimental method of virtual photon scattering can be treated as Coulomb excitation of the projectile followed by its subsequent ground-state photon decay [7,8]. The cross section for this process increases with the charge of the target and the beam energy of the projectile. In order to discriminate against nuclear processes it is necessary to limit detection of scattered projectiles to a small forward cone (selecting only large impact parameters).

There are two main differences between virtual photon absorption and virtual photon scattering. The absorption measurement cannot distinguish between different virtual photon multipolarities, whereas the scattering experiments, with the requirement of observing ground state γ-ray decays, essentially limit the virtual spectrum to $E1$ multipolarity. The

second difference is related to the neutron binding energy. As mentioned above, the absorption experiments rely on detection of neutrons for a kinematic reconstruction of the excitation energy and are therefore limited to probing strength functions above the neutron separation energy. In the scattering case, the cross section for ground-state γ-ray decay drops dramatically above the neutron binding energy. This effect, compounded further by low beam intensities, presently limits the realm of this method to excitation energies below the neutron binding energy. The neutron binding energy for ^{20}O lies at 7.608 MeV [9] which is sufficiently high to observe shifted, low-lying $E1$ strength.

3. MEASUREMENT

The measurement was performed at the National Superconducting Cyclotron Laboratory at Michigan State University. A 10^6 pps, 100 MeV/u beam of ^{20}O (produced via fragmentation of ^{22}Ne on Be) was impinged on a 30 mg/cm^2 ^{208}Pb target. This target thickness was choosen as a compromise between maximizing event rate while limiting projectile energy straggling to $\approx$ 1 MeV FWHM.

The scattered projectiles were analyzed with the S800 mass spectrometer which was

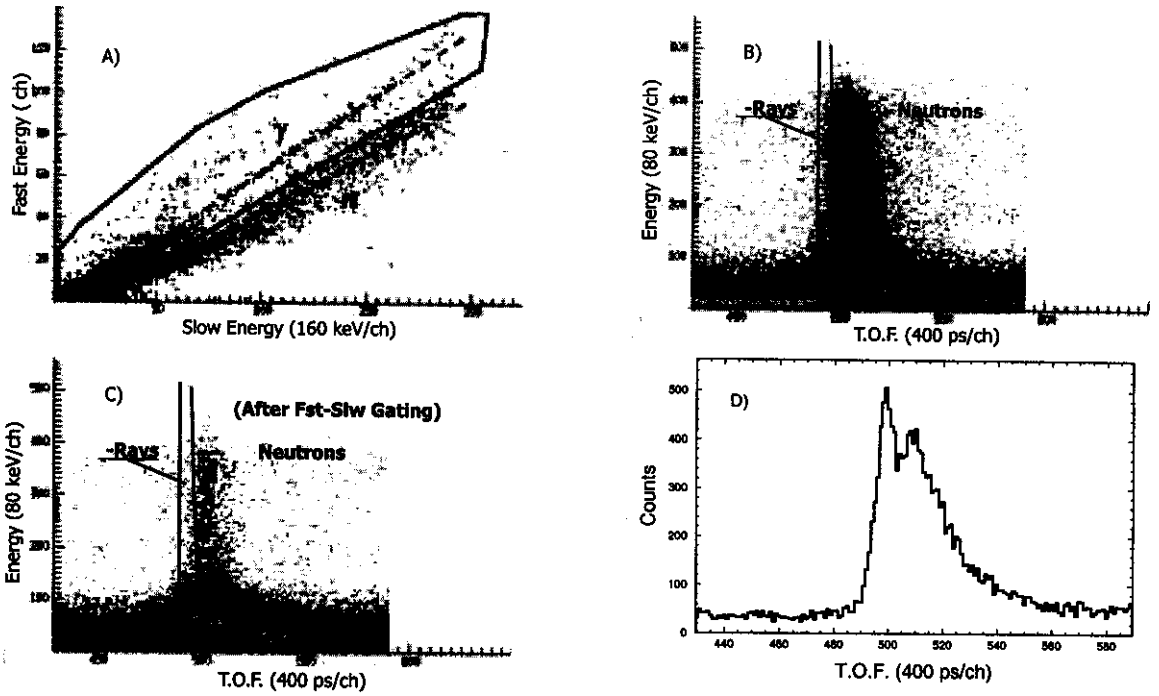

Figure 2. (A) Illustration of fast vs. slow gating. The deposited energy as detected with a short integration time ($\approx$ 50 ns) is plotted against energy with a long integration time ($\approx$ 1500 ns). (B) Time-of-flight (T.O.F.) is shown against deposited energy. (C) Same as (B) after fast vs. slow gating. (D) Projection of a 3.2–4.0 MeV energy cut from (C) on the T.O.F. axis.

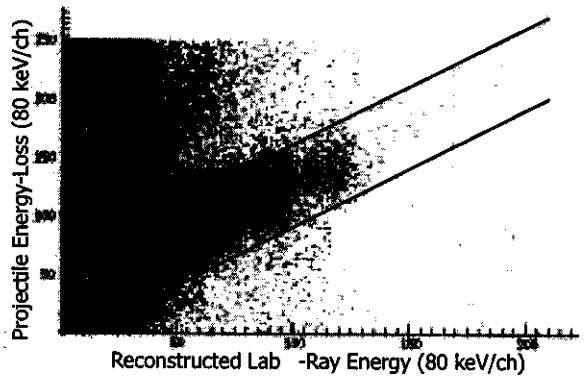

Figure 3. Final coincident event selection. Projectile energy-loss is shown against the reconstructed, lab-frame γ-ray energy. Events which are constrained by conservation of total energy fall on the diagonal.

operated in dispersion-matched mode. The standard S800 focal plane setup [10] consists of a pair of position-sensitive Cathode Readout Drift Chamber (CRDC) detectors for fragment position and tracking, a multi-segmented Ion Chamber (IC) gas detector for a multi-sampled determination of the fragment's energy-loss. Fragment identification and timing was provided by a large area, stopping scintillator. The inelastically-scattered ^{20}O projectiles were fully-separated from other reaction fragments across a range in energy-loss of $\approx$ 40 MeV.

In coincidence with the ^{20}O fragments, γ-rays were detected using 144 elements from the ORNL-TAMU-MSU BaF_2 array placed at forward angles surrounding the beam pipe, in a hexagonally-concentric orientation. The lab-frame angular coverage of the BaF_2 array was 11°–48°. For purposes of monitoring the contribution of target γ-rays to the overall yield, a smaller BaF_2 array (consisting of 7 elements) was placed at a backward location.

The placement of the detectors at very forward angles resulted in a large high-energy neutron background. Two methods where used in conjunction to suppress this neutron contamination. For neutrons depositing more than 3 MeV, "fast vs slow" gating can be applied (as shown in Figure 2(a)). This process benefits from the component of fast ultra-violet light (subnanosecond) which is emitted by BaF_2 crystals during interactions with fast electrons and therefore is dependent on the type of incident radiation [11,12]. This fast component of light emitted by BaF_2 also allowed for a prompt timing measurement, which, when coupled with the precise projectile timing provided by two well separated ($\approx$ 44 m) upstream multi-channel-plate timing detectors [13], faciliated further neutron supression via time-of-flight, see Figure 2(b,c,d).

For the selected γ-ray-coincident events, measured γ-ray energies were subjected to an add-back process, whereby energy deposited simultaneously in neighboring detectors was summed. This technique is necessary for the reconstruction of events where energy escapes detectors as a result of compton scattering and/or pair production. This technique improves the energy response of the array and the pile-up probability remains small due to the low multiplicity of multiple detector events. The summed γ-ray energy was then

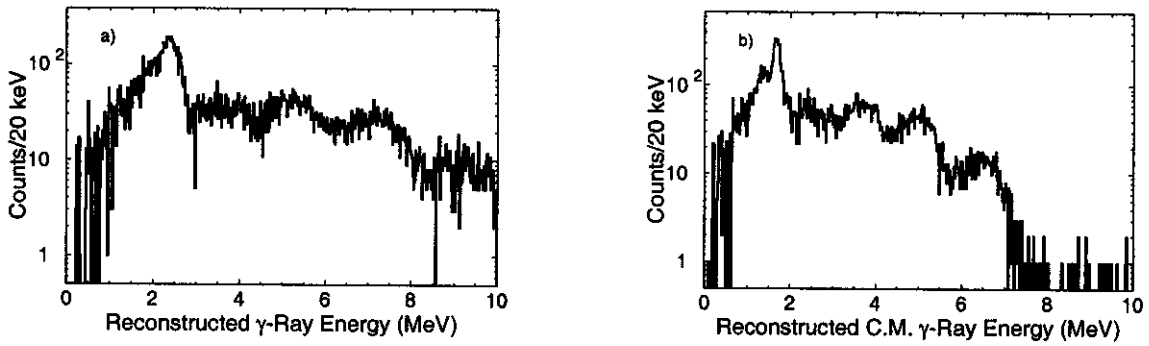

Figure 4. Reconstructed γ-ray energy spectra for all selected events: (a) represents lab-frame energy, while (b) is the Doppler-corrected equivalent. Several broad peaks are observed in the region beyond the predominant 2^+ transition at ≈ 1.7 MeV.

Doppler-corrected based on the scattering angle of the detector registering the largest energy deposition.

The final event selection required correlating projectile inelastic energy-loss, as measured by the S800, with the reconstructed γ-ray energy as shown in Figure 3. Lying along the enhanced diagonal band are events where the energy-loss is equal to the γ-ray energy, thereby fulfilling the condition for virtual photon scattering.

4. PRELIMINARY RESULTS

The preliminary results after final event-selection (the diagonal cut in Figure 3) are shown in Figure 4. This figure displays the reconstructed γ-ray energies, without (a) and with (b) Doppler correction. The pronounced peak at ≈ 1.7 MeV results from the decay of the known first-excited 2^+ state [9]. The observation of this peak is evidence for correct identification of the projectile (^{20}O). Furthermore, the sharpening of this transition when comparing Figure 4(b) against (a) is a quantitative verification of the Doppler correction process.

Several broader peaks are observed above 3 MeV. We speculate that these structures result from $E1$ strength based on theoretical $B(E1)$ and $B(E2)$ information [14,15] and approximate Coulomb excitation cross section calculations for this energy region. These broad peaks cannot correspond to incorrectly Doppler-corrected, singular, sharp peaks because these structures are even broader in the non-Doppler-corrected spectrum. Current ^{20}O experimental data reveal no information regarding discrete 1^- states below the neutron separation energy [9].

Further analysis has to be performed to decisively determine the nature of these broad structures. For example, the shower multiplicity will show if the projectiles decay directly to the ground state (in support of $E1$ multipolarity) or if a cascade through one or more transition(s) occurs. Preliminary multiplicity investigations show that these are indeed direct ground-state transitions. GEANT [16] simulations are now being performed to include the detector acceptances, efficiencies and responses.

5. CONCLUSIONS

We have performed an experiment to study low-lying GDR strength in neutron-rich ^{20}O. The preliminary excitation energy spectrum reveals several broad peaks below the neutron separation threshold which are likely of dipole multipolarity. This first virtual photon scattering experiment of β-unstable nuclei with bound excited states showed the feasibility of the method. Future radioactive beam facilities with the capability of more intense, high-energy beams will be able to apply this method to heavier and/or more neutron-rich nuclei [17]. Because the excitation cross section increases with beam energy as well as with the Z of the projectile, in heavier nuclei it will be possible to extend the observation of $E1$ strength to energies above the neutron binding energy.

ACKNOWLEDGEMENTS

This work is supported in part by the National Science Foundation grant number PHY95-28844. Oak Ridge National Laboratory is managed by UT-Battelle, LLC, for the U.S. Department of Energy under contract DE-AC05-00OR22725.

REFERENCES

1. I. Hamamoto, H. Sagawa, and X. Z. Zhang, Phys. Rev. **C53** (1996) 765.
2. I. Hamamoto, and H. Sagawa, Phys. Rev. **C53** (1996) R1492.
3. S. S. Dietrich and B. L. Berman, At. Data Nucl. Tables, **38** (1988) 199.
4. T. Aumann, *et al.*, Nucl. Phys. **A649**, 297c (1999).
5. T. Aumann, *et al.*, Phys. Rev. **C59**, 1252 (1999).
6. R. L. Varner, *et al.*, Proc. Inter. Workshop on Collective Excitations in Fermi and Bose Systems, edited by C. Bertulani, World Scientific, p.264 (1999).
7. C. A. Bertulani and A. M. Nathan, Nucl. Phys **A554** (1993) 158.
8. R. L. Varner *et al.*, Proc. 2^{nd} Inter. Conf. on Exotic Nuclei and Atomic Masses, edited by B. M. Sherrill, D. J. Morrissey, and C. N. Davids, AIP Conference Proceedings **455**, p. 245 (1998)
9. D. R. Tilley *et al.*, Nucl. Phys **A636** (1998) 249.
10. J. Yurkon *et al.*, Nucl. Instr. and Meth. **A422** (1999) 291.
11. M. Laval *et al.*, Nucl. Instr. and Meth. **206** (1983) 169.
12. R. Novotny *et al.*, Nucl. Instr. and Meth. **A262** (1987) 340.
13. D. Shapira and T. A. Lewis, to be published.
14. H. Sagawa and Toshio Suzuki, Phys. Rev. **C59** (1999) 3116.
15. E. Khan and Nguyen Van Giai, Phys. Lett. **B472** (2000) 253.
16. *Geant – Detector Description and Simulation Tool*, Application Software Group, Computing and Networks Division, CERN, Geneva, Switzerland (1993).
17. *Scientific Opportunities with Fast Fragmentation Beams from the Rare Isotope Accelerator*, NSCL Report, Michigan State University, March 2000.